Pb nanowires on vicinal Si(111) surfaces: Effects of refacetting on transport

C. Tegenkamp, D. Lükermann, S. Akbari, M. Czubanowski, A. Schuster, and H. Pfnür
Institut für Festkörperphysik, Leibniz-Universität Hannover, Appelstrasse 2, D-30167 Hannover, Germany
(Received 14 September 2010; published 10 November 2010)

The conductance of Pb wires grown by self-assembly on Si(557) has been studied in detail as a function of coverage and of the facet structure. Only for 1.31 ML, corresponding to one physical monolayer on the terraces (steps not covered with Pb), *and* a perfectly ordered wire array along the $[\bar{1}\bar{1}2]$ direction quasi-one-dimensional (1D) transport along the $[1\bar{1}0]$ direction is found, corroborating the model of one-dimensional band filling in an adsorbate induced (223) facet structure. The transport results recently shown by Morikawa *et al.* [Phys. Rev. B **82**, 045423 (2010)] can also reproduced by our group. In contrast to what was claimed by them, our results clearly show that either a too small coverage or structural imperfections of the surface are responsible for a metal-insulator transition around 140 K irrespective of the crystallographic direction. The variety of different transport scenarios found is caused by strong adsorbate-induced refacetting into an electronically stabilized (223) orientation, which differs from the macrosocopic orientation of the substrate. The crucial interplay between structure and filling factor explains the extremely small parameter window in which the 1D transport channel can be observed.

DOI: 10.1103/PhysRevB.82.205413 PACS number(s): 68.55.J−, 73.50.−h, 73.61.−r

I. INTRODUCTION

Electronic correlations play a major role in the physics of low-dimensional systems. They are of fundamental interest since they cause strong deviations from simple Fermi-liquid behavior. Among other experimental possibilities for their realization, metallic monolayers (MLs) and films grown on semiconductor surfaces were shown to be promising model systems of strongly confined electron gases that indeed exhibit such correlation effects.[1,2] The intense research on these systems is triggered by the possibility of a comprehensive characterization and selective manipulation of these structures with a variety of techniques.[3–5] Particularly, surface transport came recently in the focus of research since this method can probe inherent electronic instabilities in these low-dimensional structures directly.[6–9]

The ultimate realization of an atomic wire can be done only by using well established concepts of self-assembly. While this approach works reliably on atomic length scales, long-range ordering is still demanding. However, this is a necessary prerequisite for transport measurements as these are not performed on an atomic scale. To some extent, this problem can be overcome using Si substrates as essentially the high step stiffness[10] makes them ideal templates for growing comparably long-range ordered arrays of metallic quantum wires. But still, the morphology needs to be controlled on a large scale with atomic resolution. Though vicinal substrates allows the growth of single domain structures, these high index surfaces easily undergo refacetting processes, e.g., as reported recently for Au submonolayer coverages grown on vicinal Si(111) surfaces.[11]

The Pb/Si(557) system reveals many intriguing and novel phenomena. We have recently shown, that Pb grows layer by layer from the beginning despite of a lattice mismatch of around 9%. The lateral strain is released due to the high step density of around 20% on the Si(557) surface.[12] If adsorption is performed at elevated temperatures, the surface refacets into a (223) facet structure for coverages around one physical ML. Particularly, the 1.31 ML phase [concentration measured with respect to the Si(111) surface atom density] undergoes a temperature driven semiconductor-insulator transition in the direction perpendicular to the steps while along the steps a semiconductor-metal transition occurs by lowering of the temperature.[8,13] The transition in the $[\bar{1}\bar{1}2]$ direction was assigned to nesting of the electronic structure in this direction. While this transport signature depends sensitively on coverage and the homogeneity of the sample, the formation of (223) facets depends only marginally on the exact overage.[14,15] From a crystallographic point of view, the Pb-induced formation of (223) facets instead of a (557) orientation is surprising and thus gives direct evidence for the pronounced coupling of the wires and for the importance of the electronic structure of the surface states.

Recently performed transport studies by Morikawa *et al.*,[16] using a microscopic, colinear four-point probe (μ−4PP) reveal a the transition from metal to insulator below 140 K but not to a 1D metallic state as found by us. This motivated us to further investigations about the possible origin for this discrepancy. Our results demonstrate clearly that imperfections, i.e., nonpercolated electron paths on a mesoscopic scale, can indeed give rise to such transitions. For transport measurements extended metallic states are necessary. This makes the anticipation of a certain transport behavior on the basis of solely spectroscopic data extremely dangerous. In this paper we will show how structure and conductance are modified by small changes in Pb concentration, as expected in an in principle two dimensional, although anisotropic, electronic system with one-dimensional properties only when specific conditions like 1D band filling are fulfilled. It is obvious that under these conditions also defects, particularly those on a mesoscopic scale, will play a major role as well. Therefore, the impact of such defects on surface sensitive transport measurements is presented and discussed.

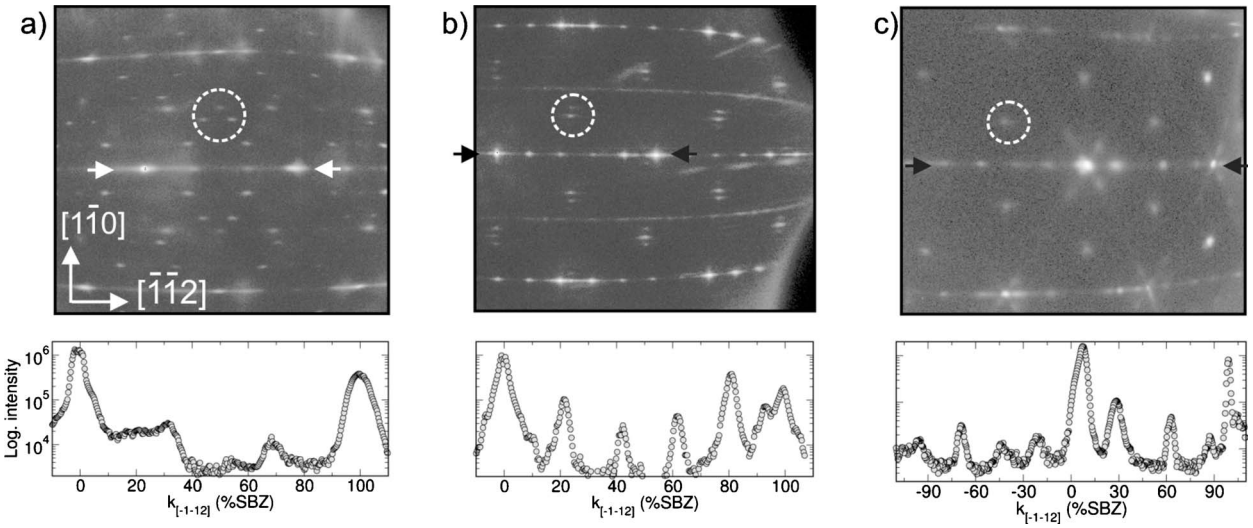

FIG. 1. Series of LEED patterns of Pb/Si(557) of different coverages and structural order: (a) Pb coverage 1.2 ML and [(b) and (c)] 1.3 ML. The line scans were taken along the [$\bar{1}\bar{1}$2] direction, as indicated by the arrows. Only in (b) a perfect (223) facet orientation is obvious while in the other cases either the coverage is too low (a) or excessive thermal treatment (c) causes imperfect step trains. The circles show the typical Pb-induced reconstructions which allow the accurate determination of the Pb coverage. The crystallographic directions are given with respect to Si(111) terraces. All LEED patterns were taken at temperatures below 78 K and at an electron energy of 99 eV.

II. EXPERIMENTAL SETUP

Low-doped Si(557) samples (size 15×15 mm^2, resistivity ≥1000 Ω cm) with eight $TiSi_2$ contacts have been used to perform simultaneous low-energy electron diffraction (LEED) and macroscopic four-point conductance measurements both parallel and perpendicular to the wirelike structures obtained by monolayer Pb films on vicinal Si(557). The contacts were fabricated by evaporation of Ti on HF-dipped samples in a vacuum of 10^{-6} mbar at elevated temperatures between 700 and 800 °C. Afterward the samples were mounted on the sample holder and transferred into the main UHV chamber (base pressure 1×10^{-10} mbar). Crystalline and perfectly stepped Si surfaces were obtained by subsequent e-beam heating of the samples to temperatures of 1100 °C. The morphology was controlled in detail by spot profile analysis (SPA) LEED. The LEED analysis of many samples has shown that refacetting easily occurs if higher substrate temperatures were used. The specifics of diffraction patterns for perfectly ordered Si(557) surfaces were already discussed previously.[14]

Pb was evaporated out of a ceramic crucible and the amount was controlled by a quartz microbalance. The monolayer phases were formed by annealing the sample to 640 K. The transport properties and also the facet structures depend crucially on the exact Pb coverage. As we will show below the splitting of spots stemming from both the step train and the $\sqrt{3}$ reconstruction were used in order to measure the Pb coverage with high accuracy. Further details about the preparation have been reported elsewhere.[14,17] All coverages are given with respect to the atomic density on the Si(111) surface, i.e., for a physically closed monolayer film 1.33 ML are needed ($1\ \text{ML}=7.83\times10^{14}1/\text{cm}^2$). The samples were cooled during measurements by a cryostat with a temperature range between 4 K (with cooled radiation shield) and 300 K. The temperature was measured by a Si diode mounted on the cryostat itself and was calibrated using dummy samples with thermocouples.

III. RESULTS AND DISCUSSION

A. Refacetting vs homogeneity

Vicinal substrates are per se metastable and tend to refacet, especially, if the energetics of step formation are changed, e.g., by adsorption or externally applied stress.[11] The Pb/Si(557) system is such an example, which shows many different Pb monolayer phases and facet structures depending on the Pb coverage and thermal treatment. Not surprisingly, it turns out, that this morphology, both as periodic arrays or as nonperiodic step bunches, plays a crucial role on electrical conductance in the monolayer regime. Figure 1 shows exemplarily three LEED patterns of surface structures induced by a Pb concentration close to one physical monolayer on the terraces. For these LEED patterns the Pb concentration differs by less than 10%, but this has strong implications on morphology and electronic transport, as will be shown.

The LEED pattern shown in Fig. 1(a) is found at a coverage close to 1.2 ML. As judged by the spot splitting along the [$\bar{1}\bar{1}$2] direction of 37% surface Brillouin zone (SBZ), the dominant periodic structure on this surface consists of (112) facets. The width of the facets is around 35 Å, as deduced from the full width at half maximum of the facet peaks at an out-of-phase condition. The symmetrically split spot structure around the $\sqrt{3}$ positions is due to formation of $\sqrt{7}\times\sqrt{3}$ reconstructions on wider (111) terraces. A detailed analysis of this phase as well as a detailed description of the clean Si(557) surface can be found in Ref. 14. Thus the former alternating arrangement of (111) and (112) facets of the clean

surface is annihilated after Pb adsorption and transformed into a surface with large bunches of these units. Along with the formation of the Pb reconstructions the step energetics are changed so that a new nonhomogenously stepped surface is generated. In the particular case shown in Fig. 1(a) the (112) facets must be separated by nonperiodic (111) facets or, more efficiently, by upward steps (steps in opposite direction than that given by the vicinality of the surface) in between in order to maintain the overall vicinality of the sample.

The small increase in Pb concentration to 1.3 ML results in a much more homogeneous surface but also in formation of a different facet orientation. The LEED pattern now shows a characteristic spot splitting along the $[\bar{1}\bar{1}2]$ direction of 21.3% SBZ [see Fig. 1(b)]. This spot splitting is an indication of (223) facet formation, and is most likely electronically stabilized by this and higher Pb concentrations, as concluded from angle resolved photoelectron spectroscopy (ARPES) measurements.[18] This electronic stabilization has the consequence of a high sensitivity of electronic properties to structural details and homogeneity, as we will show below. One of these structural details is the spot splitting of 10% SBZ along the miniterraces ($[1\bar{1}0]$) caused by a sequence of five $\sqrt{3}\times\sqrt{3}$ unit cells separated by a $\sqrt{7}\times\sqrt{3}$ domain wall. This tenfold periodicity is important in order to explain the split-off states found in spectroscopy,[18] which leads to high conductance at low temperature. However, they are not directly relevant for the Fermi nesting in the $[\bar{1}\bar{1}2]$ direction. Therefore, we will concentrate in the following essentially on the latter direction. The splitting of the $\sqrt{3}$ reflexes, which is the 1D analog of the devil staircase phases found for Pb/Si(111),[19] has been used in order to determine the exact coverage with high precision ($\Delta\Theta\approx 0.01$ ML).[14,20] In order to maintain the inclination of the former Si(557) substrate, a small concentration of nonperiodically arranged (111) terraces or of facets with opposite inclination must be present again. However, these features are not seen by LEED, but an increase in their concentration, which is then visible in LEED, has dramatic consequences for macroscopic transport measurements (see below).

For coverages in between 1.2 and 1.31 ML, different facet orientations have been found.[14] For instance, the adsorption of 1.24 ML Pb has revealed a spot splitting along the $[\bar{1}\bar{1}2]$ direction which corresponds to a (335) facet structure. If the coverage is slightly higher but still below 1.3 ML, the (223) facets coexist with other orientations. The details about the exact distribution of different coexisting facet structures depend of course strongly on the history of the sample.

Since the (223) facet structure is only stabilized by the opening of a small band gap,[18] it can easily distorted, e.g., by external stress or surface impurities. Two examples, where the total Pb coverage is identical to the "optimal" 1.31 ML of Pb are shown exemplarily in Figs. 2(b) and 1(c), where the maximum annealing temperature prior to the deposition of Pb was gradually increased to 1470 K and 1520 K, respectively. While in Fig. 2(b) most of the fingerprints seen in Fig. 1(b) are present, i.e., domain wall splitting of the Pb reconstruction and streaks along the half order position due to dimerization at step edges, in Fig. 1(c) even the (223) reconstruction is not obvious from the LEED pattern any more. Instead, the splitting is around 30% SBZ, similarly to the structure shown in Fig. 1(a), but the initial coverage is higher than in Fig. 1(a) as obvious from the appearance of reconstruction spots at only $\sqrt{3}$ positions. Besides this it is also evident that the intensity of the LEED pattern itself is not homogenously distributed. As the spot size of our LEED instrument is finite (1 mm), we incoherently average over many different atomic configurations on the sample. In this sense, LEED is a powerful tool to obtain information on a macroscopic scale.

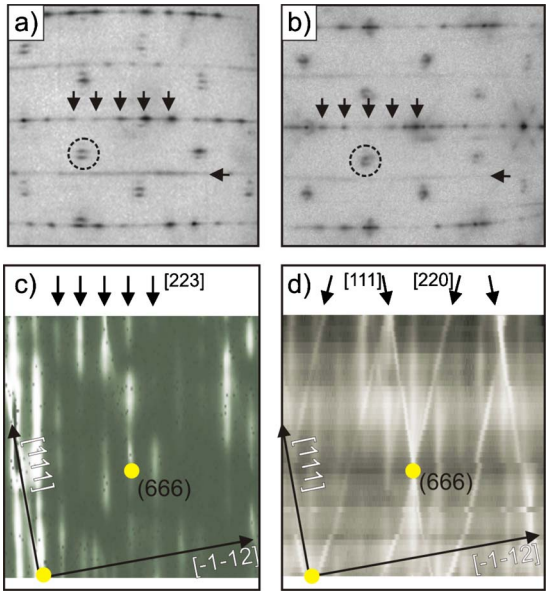

FIG. 2. (Color online) [(a) and (b)] LEED pattern taken at 99 eV with coverage of 1.3 ML. (c) and (d) show the $(k_\perp, k_\parallel)$ plots for (a) and (b), respectively ($T=70$ K). Bulk Bragg peaks are marked by solid circles. The arrows mark the positions of the (223) facet rods in (c) while in (d) also (111) and (220) rods are visible.

In some cases the signatures for refacetting of the surface are extremely faint and are close to the resolution limit of the LEED instrument. For instance, the two LEED patterns shown in Figs. 2(a) and 2(b) look quite similar revealing both the characteristic spot splittings along both directions (marked by circles and arrows) as characteristic for perfectly grown Pb wires. However, Fig. 2(b) is strongly refacetted. This comes out more clearly when line scans taken along the $[\bar{1}\bar{1}2]$ direction for various electron energies are plotted intensity coded in a $(k_\perp, k_\parallel)$ plot. Besides the (223) facet structure, facet rods are visible running along the [111] and [220] directions. On the contrary, the corresponding $(k_\perp, k_\parallel)$ plot of Fig. 2(a) shown in Fig. 2(c) shows only the (223) facet rods. As we will show below only the latter shows the intriguing 1D-transport behavior.

B. Surface transport

We will focus now on surface transport and want to address two main aspects: the sensitivity to exact Pb concentration for the observed conductance as a function of temperature and the effect of surface inhomogeneities. Starting

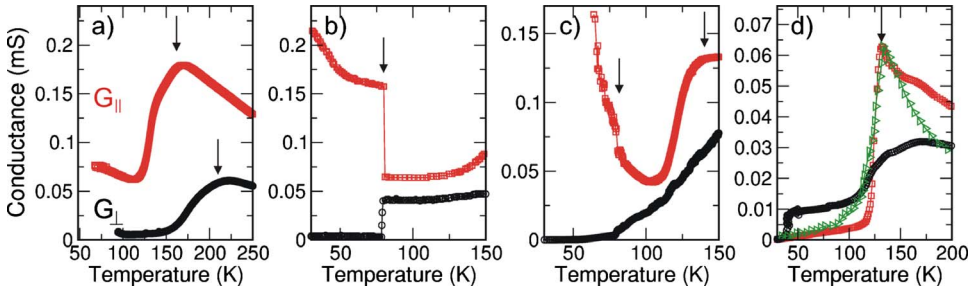

FIG. 3. (Color online) Conductance curves of Pb phases along $[G_{\|}$ (red) squares] and perpendicular $[G_{\perp}$ (black) circles] to the step direction for various Pb coverages and surface homogeneities. Conductance of annealed 1.27 ML of Pb (a), of 1.31 ML (b) with metal-insulator transitions along both directions at 78 K. If the coverage is slightly higher (c, 1.32 ML), the 1D/2D transition is only barely visible while indications for the transition around 140 K appear again. (d) Conductance of 1.31 ML of Pb on strongly facetted surface. The arrows indicate the different transition temperatures. The (green) triangles show (scaled) data derived from Ref. 16.

with the quasiperfect and completely Pb covered (223) facet structure (1.31 ML), 1D transport is found at low temperatures as demonstrated in Fig. 3(b). Below 78 K the system switches reversibly into a 1D regime, where only along the wires transport occurs while in the $[\bar{1}\bar{1}2]$ direction the conductance is almost zero and essentially limited by the residual conductance of the substrate. We have recently shown that this switching in transport is coupled with a refacetting structural transition.[21] The origin of the 1D transport regime has been explained by Fermi nesting, i.e., coincidence of twice the Fermi wave vector and the reciprocal lattice vector leading to localization. The delocalized channel along the wires is the result of split-off states, which intersect the Fermi surface close to the center of the Brillouin zone.[18] These states most likely originate from spin-orbit coupling, as suggested by recent magnetotransport results.[17] The signature in LEED is the spot splitting around the $\sqrt{3}$ positions along the $[\bar{1}\bar{1}2]$ direction [cf. with Figs. 1(b) and 2(a)].

In order to have Fermi nesting, the mutual relation between band structure and band filling is extremely strict. As a consequence, deviations from the optimal coverage strongly influence the conductance properties, most visible in the temperature-dependent conductance. This is demonstrated in Fig. 3(c) by the increase in coverage by one to two hundreds of a monolayer above the optimal coverage. The 1D/two-dimensional (2D) transition, although still visible as well as the delocalized state along the wire, is strongly damped. Furthermore strong increase around 140 K becomes dominant in the direction along the wires, which turns out to be a characteristic signature of localization due to imperfections.

Similarly, if band filling is not complete, as for the case of 1.27 ML [see Fig. 3(a)], strong changes in the absolute values and even more in the temperature dependence of conductance are observed compared with the 1.31 ML case. Most importantly, the temperature dependence of conductance is reversed for the direction parallel to the wires, i.e., we see a classical metal-insulator transition at low temperatures in both directions. In both directions the conductance now increases strongly with increasing temperature, still with a clear anisotropy, i.e., the conductance along the wires remains higher than in the $[\bar{1}\bar{1}2]$ direction. These conductance curves are characteristic for activated transport and, evidently, the activation along the two crystallographic directions is different. While along the wires the transition temperature is around 140 K, the onset of conductance across the wires is around 220 K. The latter behavior is expected if the space charge layer of the Si surface, i.e., the change in the chemical potential due to thermal ionization of the dopants, is largely contributing.[22] This is compatible with the structural model of incomplete filling of the terraces deduced in context with Fig. 1(a), resulting in stronger electronic separation of the individual wires. Thus activation of charge carriers in the Si surface layer dominates electronic transport perpendicular to the wires. Along the wire direction Pb-induced reconstructions and there formation with defects due to incomplete filling yield again an activation barrier, which, however, is considerably smaller than in the $[\bar{1}\bar{1}2]$ direction. The residual imperfections along this direction suppress any highly conductive state below 140 K. It should be mentioned that in contrast to the 1.31 ML phase presented above, no structural phase transitions were observed by LEED at this Pb coverage.

On the other hand, if a full physical monolayer is deposited on a strongly refacetted surface, as generated by flash cycles to too high temperatures [1450 K, Fig. 3(d)], again only activated transport behavior is found. The conductance maxima are now observed at 140 K in both directions, and the initial conductance at low temperatures has decreased by more than one order of magnitude in $[1\bar{1}0]$ direction. Please note that in this case the surface is, at least on the length scale relevant for transport measurements, homogeneously covered with the optimal 1.31 ML Pb concentration. Therefore, the metal-insulator transitions appear at identical temperatures in both directions in contrast to the 1.27 ML case discussed above. An anisotropy of the surface remains with a higher conductance along the wires above 120 K. The suppression of the delocalized transport channel at low temperatures is in agreement with the absence of the spot splitting of the corresponding LEED structure [cf. Fig. 1(c)]. Moreover, structural changes were again not found as a function of temperature, i.e., this metal-insulator transition is fundamentally different from that seen at 78 K for the perfectly ordered Pb wire system. It is interesting to note that the conductance measured along the step direction is, after simple scaling, identical to that measured by Morikawa *et al.*[16] [data are shown as triangles in Fig. 3(d)].

Although not all details of the conductance curves can yet be correlated with the precise morphological properties, our

findings lead to the following conclusions: the 1D transport channel shown in Fig. 3(b) is unambiguously related to a long-range ordered wire structure *and* a correct Pb coverage. This mutual relation between band filling and band structure was identified as Fermi nesting in spectroscopy.[18] The peculiar properties of the Pb-induced (223) structure are fully supported by latest SPA-LEED investigations showing a refacetting transition at exactly 78 K (Ref. 21) and the formation of Pb superlattices atop the (223) facet[20] as a function of temperature and excess coverage, respectively. Recently performed magnetotransport measurements have shown further that the spin-orbit coupling is strongly suppressed for this 1.31 ML phase.[17]

Exceeding the exact coverage of 1.31 ML has another interesting aspect as revealed by a recent high-resolution LEED experiment. By adsorption of excess coverage, the steps of the (223) facet get decorated by atomic chains. This edge filling does not occur randomly but results in additional superperiodicities perpendicular to the step edges with extremely large lattice constants (up to 10 nm).[20] Interestingly, the underlying (223) facet structure (measured below 78 K) remains intact. Therefore, the formation of these superstructures was again postulated to be electronically stabilized by formation and filling of new subbands within the existing gap of 20 meV visible at 1.31 ML Pb coverage.[23] If this model is correct, the surface must remain insulating in the $[\bar{1}\bar{1}2]$ direction at Pb coverages higher than 1.31 ML but with effectively decreasing activation energies as a function of increasing Pb concentration. This is exactly what we find here for the conductance in $[\bar{1}\bar{1}2]$ direction (see Fig. 4). Starting from 1.31 ML of Pb with the small gap of around 20 meV,[18] the 1.32 ML curve still shows the abrupt transition, which apparently has disappeared for 0.06 ML Pb excess coverage. At the same time, the original insulating state below 78 K becomes more and more conducting as the coverage is increased with clear activated behavior. The quantitative evaluation from the right part of this figure, shown in the inset, indeed reveals a continuously decreasing effective activation barrier for electronic transport, which ends in purely metallic behavior at a Pb concentration of 1.50 ML. Thus, interpreting these activation energies ΔE as the gradual decrease in the band gap, these findings from transport nicely fits into the nesting model (see inset of Fig. 4). Once 1.5 ML is deposited, all steps are completely decorated, and fully metallicity is reached, as expected.[14] At this concentration the physical monolayer is completed.

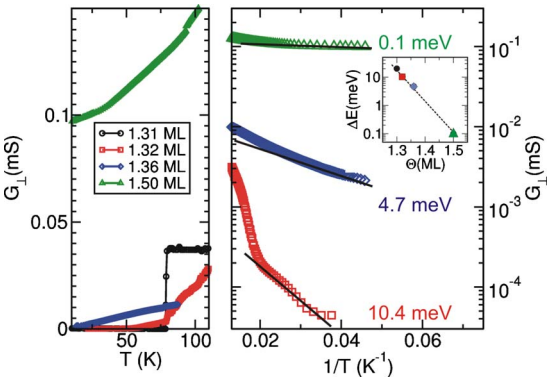

FIG. 4. (Color online) Temperature dependence of conductance $G_\perp$ across the wires for various Pb coverages between 1.3 and 1.5 ML on almost perfect (223) templates on linear scale (left) and as semilog plot versus $1/T$ (right). The inset shows the effective activation energies ΔE for electronic transport derived from these data and that obtained from ARPES (black circle).For further details see text.

IV. CONCLUSION

In summary, we have shown that the Pb monolayer system on Si(557) has indeed to be considered as an anisotropic, but clearly two-dimensional electronic system, also close to the Fermi level. In such a system, anisotropy can lead to anisotropic band filling at certain points of coverage. Such a limiting behavior was found as one-dimensional conductance for the concentration of 1.31 ML of Pb, which here is assisted by Pb-induced refacetting. It is an obvious consequence of this physical scenario that such properties are very susceptible to small distortions both in Pb concentration and by the morphology of the substrate. This was shown by our set of experiments presented here. Thus we were also able to quantitatively reproduce the data by Morikawa *et al.*,[16] which show the typical signature of a defected surface. The defects suppress all phase transitions, as demonstrated by us. Therefore, it is not surprising that the 1D-2D conductance phase transitions was not seen by this group.

On the other hand, excess coverage not only acts as defects but introduces new physical scenarios, as shown for Pb excess coverages up to 1.50 ML. Step decoration and the occurrence of new subbands in the band gap that stabilizes the 1D conducting properties leads to a sequence of new periodicities with more and more shrinking effective band gaps until, at a coverage of 1.50 ML, all steps are completely decorated and band gaps disappear, resulting in purely metallic behavior.

ACKNOWLEDGMENTS

Financial support by the Deutsche Forschungsgemeinschaft is gratefully acknowledged.

[1] J. Schäfer, C. Blumenstein, S. Meyer, M. Wisniewski, and R. Claessen, Phys. Rev. Lett. **101**, 236802 (2008).

[2] C. Brun, I.-Po Hong, F. Patthey, I. Y. Sklyadneva, R. Heid, P. M. Echenique, K. P. Bohnen, E. V. Chulkov, and W. D. Schneider, Phys. Rev. Lett. **102**, 207002 (2009).

[3] J. N. Crain, A. Kirakosian, K. N. Altmann, C. Bromberger, S. C. Erwin, J. L. McChesney, J. L. Lin, and F. J. Himpsel, Phys. Rev. Lett. **90**, 176805 (2003).

[4] H. W. Yeom, S. Takeda, E. Rotenberg, I. Matsuda, K. Horikoshi, J. Schaefer, C. M. Lee, S. D. Kevan, T. Ohta, T. Nagao, and S.

Hasegawa, Phys. Rev. Lett. **82**, 4898 (1999).
[5] J. R. Ahn, P. G. Kang, K. D. Ryang, and H. W. Yeom, Phys. Rev. Lett. **95**, 196402 (2005).
[6] T. Kanagawa, R. Hobara, I. Matsuda, T. Tanikawa, A. Natori, and S. Hasegawa, Phys. Rev. Lett. **91**, 036805 (2003).
[7] S. Hasegawa, I. Shiraki, F. Tanabe, R. Hobara, T. Kanagawa, T. Tanikawa, I. Matsuda, C. L. Petersen, T. M. Hansen, P. Boggild, and F. Grey, Surf. Rev. Lett. **10**, 963 (2003).
[8] C. Tegenkamp, Z. Kallassy, H. Pfnür, H.-L. Günter, V. Zielasek, and M. Henzler, Phys. Rev. Lett. **95**, 176804 (2005).
[9] Ph. Hofmann and J. W. Wells, J. Phys.: Condens. Matter **21**, 013003 (2009).
[10] H. C. Jeong and E. D. Williams, Surf. Sci. Rep. **34**, 171 (1999).
[11] I. Barke, F. Zheng, S. Bockenhauer, K. Sell, V. v. Oeynhausen, K. H. Meiwes-Broer, S. C. Erwin, and F. J. Himpsel, Phys. Rev. B **79**, 155301 (2009).
[12] D. Lükermann, H. Pfnür, and C. Tegenkamp, Phys. Rev. B **82**, 045401 (2010).
[13] C. Tegenkamp, Z. Kallassy, H.-L. Günter, V. Zielasek, and H. Pfnür, Eur. Phys. J. B **43**, 557 (2005).
[14] M. Czubanowski, A. Schuster, S. Akbari, H. Pfnür, and C. Tegenkamp, New J. Phys. **9**, 338 (2007).
[15] H. Morikawa, K. S. Kim, D. Y. Jung, and H. W. Yeom, Phys. Rev. B **76**, 165406 (2007).
[16] H. Morikawa, K. S. Kim, Y. Kitaoka, T. Hirahara, S. Hasegawa, and H. W. Yeom, Phys. Rev. B **82**, 045423 (2010).
[17] D. Lükermann, M. Gauch, M. Czubanowski, H. Pfnür, and C. Tegenkamp, Phys. Rev. B **81**, 125429 (2010).
[18] C. Tegenkamp, T. Ohta, J. L. McChesney, H. Dil, E. Rotenberg, H. Pfnür, and K. Horn, Phys. Rev. Lett. **100**, 076802 (2008).
[19] M. Yakes, V. Yeh, M. Hupalo, and M. C. Tringides, Phys. Rev. B **69**, 224103 (2004).
[20] M. Czubanowski, H. Pfnür, and C. Tegenkamp, Surf. Sci. **603**, L121 (2009).
[21] M. Czubanowski, A. Schuster, H. Pfnür, and C. Tegenkamp, Phys. Rev. B **77**, 174108 (2008).
[22] J. W. Wells, J. F. Kallehauge, T. M. Hansen, and P. Hofmann, Phys. Rev. Lett. **97**, 206803 (2006).
[23] Contrary to the classical Peierls mechanism, no lattice distortion is necessary at step edges. As a consequence, no structural phase transitions are expected, and indeed were not found.